

Research Article

Synthesis of Nickel and Nickel Hydroxide Nanopowders by Simplified Chemical Reduction

Jeerapan Tientong, Stephanie Garcia, Casey R. Thurber, and Teresa D. Golden

Department of Chemistry, University of North Texas, 1155 Union Circle No. 305070, Denton, TX 76203, USA

Correspondence should be addressed to Teresa D. Golden; tgolden@unt.edu

Received 31 July 2013; Revised 3 December 2013; Accepted 4 December 2013; Published 5 February 2014

Academic Editor: Thomas Thundat

Copyright © 2014 Jeerapan Tientong et al. This is an open access article distributed under the Creative Commons Attribution License, which permits unrestricted use, distribution, and reproduction in any medium, provided the original work is properly cited.

Nickel nanopowders were synthesized by a chemical reduction of nickel ions with hydrazine hydrate at pH ~12.5. Sonication of the solutions created a temperature of 54–65°C to activate the reduction reaction of nickel nanoparticles. The solution pH affected the composition of the resulting nanoparticles. Nickel hydroxide nanoparticles were formed from an alkaline solution (pH~10) of nickel-hydrazine complexed by dropwise titration. X-ray diffraction of the powder and the analysis of the resulting Williamson-Hall plots revealed that the particle size of the powders ranged from 12 to 14 nm. Addition of polyvinylpyrrolidone into the synthesis decreased the nickel nanoparticle size to approximately 7 nm. Dynamic light scattering and scanning electron microscopy confirmed that the particles were in the nanometer range. The structure of the synthesized nickel and nickel hydroxide nanoparticles was identified by X-ray diffraction and Fourier transform infrared spectroscopy.

1. Introduction

Synthesis of metal nanoparticles or nanoclusters in powders has attracted increasing attention in recent years, due to their novel electronic, optical, and magnetic properties. These metal nanoparticles have various uses in catalysts, paints, pigments, and sensors applications [1–4]. Generally, metal nanopowders are synthesized by the reduction of metal ions in aqueous or organic solution, by a chemical reagent or electrochemical current [5]. Many other methods have been devised to synthesize these powders, including a hydrothermal reduction method [6, 7], microemulsion synthesis [8], chemical reduction at acidic pH [9], and electrochemical reduction with a rotating cathode [10]. Much focus has been on methods that allow control of the particle size as there is evidence that particle size directly affects the properties of the powder [11, 12]. Other considerations for researchers include the prevention of agglomeration and oxidation of the particles [13] and quantity synthesis with a focus on industrialization of the process [14]. Stabilizers such as polyvinylpyrrolidone (PVP) are often used for particle protection and are able to decrease particle size [15, 16].

For nickel nanoparticles, chemical synthesis using hydrazine reduction has been a successful synthesis route [17–19]. While nickel nanoparticles are advantageous for certain uses, nickel hydroxide also has many important technological uses. Nickel hydroxide is used for battery, photocatalysis, and fuel cell applications [20, 21]. Depending on the pH and other species in the solution, either nickel or nickel hydroxide particles can be formed. Therefore having a simple technique for synthesis of both is advantageous.

In this paper, we present a simple, inexpensive, and efficient chemical method of synthesizing nickel and nickel hydroxide powders with nanometer-sized particles. The synthesis uses a hydrazine reduction route taking advantage of sonication at room temperature.

2. Experimental

2.1. Materials. All chemicals were of analytical grade and used without further purification: nickel chloride ($\text{NiCl}_2 \cdot 6\text{H}_2\text{O}$) from Fisher Scientific, 98% hydrazine hydrate ($\text{N}_2\text{H}_4 \cdot \text{H}_2\text{O}$) from Aldrich, and sodium hydroxide (NaOH) from EM Science. All solutions were prepared with DI water.

2.2. Synthesis of Nickel Nanopowder. The nickel nanopowders were synthesized by reduction of nickel in an aqueous solution with hydrazine hydrate acting as the reductant. For solution A, 0.5 g of nickel chloride ($\text{NiCl}_2 \cdot 6\text{H}_2\text{O}$) was dissolved in 60 mL of distilled water. In a separate beaker, solution B was prepared by dissolving 1.0 g of NaOH in 20 mL DI water and then adding 20 mL of hydrazine hydrate. Solution B was then added to solution A; the combined solution turned into a royal blue color and was mixed with a stirring rod for 2 minutes, resulting in a pH ~ 12.5 solution. For the synthesis of nickel powder stabilized by PVP, solution B was prepared by dissolving 0.2 g of PVP in 3 mL of absolute ethanol and then slowly introduced into the NaOH solution; then hydrazine was added and the solution was stirred.

According to Chen and Zhou, the reaction temperature needs to stay below 70°C in order to prepare ultrafine nickel particles [22]. The solution was sonicated for 15 minutes to $\sim 55^\circ\text{C}$, allowed to sit for 15 minutes in order to control the temperature, and then sonicated again for 15 minutes to $\sim 65^\circ\text{C}$, to activate the precipitation of the nickel particles. During the activation period, the solution initially became grey and coated along the side and bottom of the beaker and then precipitated out to the bottom as a black powder. The nickel powder solution was centrifuged and washed with DI water and absolute ethanol and was allowed to dry at room temperature.

2.3. Synthesis of Nickel Hydroxide Nanopowder. Solution A was prepared in a 250 mL volumetric flask composed of 1.19 g of nickel chloride dissolved in 50 mL DI water; then 200 mL of absolute ethanol was added to the mark, forming a green solution. The solution was transferred into a 500 mL conical flask. Solution B was prepared in a 200 mL volumetric flask. First, 0.4 g of sodium hydroxide was dissolved in 100 mL of DI water; 1.5 mL of hydrazine hydrate was added and then diluted to the mark with DI water. Solution B was slowly dropped into solution A from a burette at a rate of ~ 0.2 mL per minute and mixed with a magnetic stirrer. The resulting solution became cloudy green with precipitate forming as soon as the pH reached 6.8 and then turned to a cloudy blue green. The mixed solution finally became a grey blue with the addition of 80–90 mL of solution B at a final pH of ~ 10 . The precipitated solution was centrifuged. The powders were washed with DI water and absolute ethanol and then freeze dried.

2.4. Characterization. X-ray diffraction scans were run on the synthesized nickel and nickel hydroxide powders with a Siemens D-500 diffractometer with Cu $K\alpha$ radiation ($\lambda = 0.15405$ nm). XRD scans were run at a step size of 0.05 degrees and dwell time of 1 s. The tube source was operated at 40 kV and 30 mA. A Williamson-Hall analysis was done on each sample to calculate the particle size with silicon powder as the standard for instrumental broadening. Dynamic light scattering (DLS) (Beckman-Coulter Delsa Nano-C) was used to determine the size of the nanoparticle colloids in aqueous solution. Each of the dried nanoparticle powders was dispersed into an aqueous environment by

sonication for 30 minutes. The samples were allowed to equilibrate for 60 seconds at 25°C using a peltier device and scanned 40 times during the analysis. The nanoparticles of the powders were characterized with a FEI Nova nanoSEM 230 scanning electron microscope (SEM) with an ETD detector. Fourier transform infrared spectroscopy (FTIR) (Perkin Elmer Spectrum One) spectra were obtained for each of the nanoparticle powders using the Attenuated Total Reflectance (ATR) attachment in the range of 450 to 4000 cm^{-1} .

3. Results and Discussion

Nickel nanoparticles were synthesized from a nickel-hydrazine mixture in a sodium hydroxide environment at high pH (~ 12.5) which is favorable to form nickel nanoparticles [18, 19]. Hydrazine (N_2H_4) has a standard reduction potential of -1.16 V in an alkaline solution, represented by the oxidation reaction ($\text{N}_2\text{H}_4 + 4\text{OH}^- = \text{N}_2 + 4\text{H}_2\text{O} + 4\text{e}^-$) when mixed with the nickel ions [18, 23]. Nickel, which has a standard reduction potential of -0.25 V , is consequently able to be reduced by hydrazine ($2\text{Ni}^{2+} + 4\text{e}^- = 2\text{Ni}$) [18]. Therefore, a chemical reduction process of the nickel ion with hydrazine as a reductant in an alkaline aqueous solution can be simply shown in the following equation: $2\text{Ni}^{2+} + \text{N}_2\text{H}_4 + 4\text{OH}^- \rightarrow 2\text{Ni} + \text{N}_2 + 4\text{H}_2\text{O}$. Solution pH influences the synthesis of the nickel nanoparticles as seen in the Nernst equation (1). The discharge of the nickel nanopowders was enhanced when the redox potential, the driving force of the reaction, increased because of the increasing pH of the solution, by adding a strong base such as sodium hydroxide at a certain temperature and constant nickel ion concentration [17–19]. In addition, it has been shown that nickel powder, a gray-black powder, cannot be produced if the pH is less than 9.5 [19]:

$$E = E^\circ - \frac{RT}{4F} \ln \frac{1}{[\text{OH}^-]^4 [\text{Ni}^{2+}]^2} \quad (1)$$

$$= E^\circ - \frac{2.303}{4F} \log \left\{ [\text{OH}^-]^4 [\text{Ni}^{2+}]^2 \right\}.$$

However, in order to avoid precipitation of hydroxide, it is crucial to maintain the reduction process at a high pH [18]. This is because the standard reduction potential of $\text{Ni}(\text{OH})_2$ is -0.72 V for $\text{Ni}(\text{OH})_2 + 2\text{e}^- = \text{Ni} + 2\text{OH}^-$.

For the synthesis of $\text{Ni}(\text{OH})_2$ nanopowder, hydrazine was slowly added dropwise into the nickel solution and gradually changed from a clear green (initial pH of 4) to a cloudy blue green when the pH reached ~ 7 . Hydrazine also acted as a ligand which was able to initially form a complex of $[\text{Ni}(\text{N}_2\text{H}_4)_2]\text{Cl}_2$, $[\text{Ni}(\text{N}_2\text{H}_4)_3]\text{Cl}_2$, or $[\text{Ni}(\text{N}_2\text{H}_4)_6]\text{Cl}_2$ in the nickel solution with respect to the molar ratio of nickel to hydrazine [18]. When the pH reached ~ 7 , the complex began to form nickel hydroxide nanoparticles where the local pH around the hydrazine-sodium hydroxide droplet environment tended to be basic. The particles were gradually created when the pH increased as a result of an enhancement of the reducing power of hydrazine [19]. The addition of the

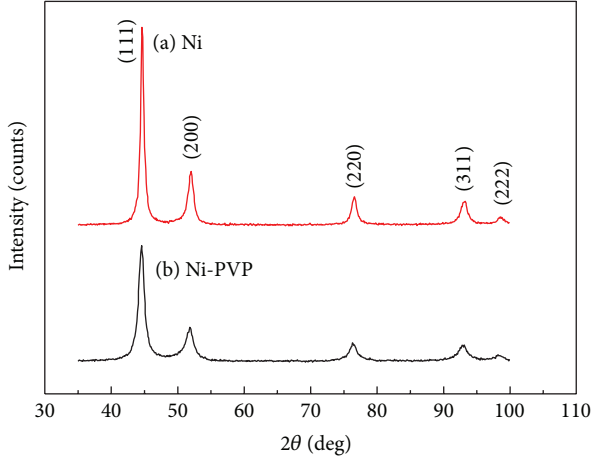
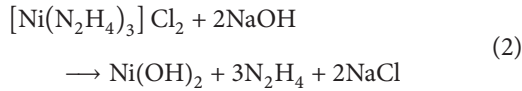


FIGURE 1: XRD pattern of (a) nickel and (b) nickel powders stabilized by PVP, precipitated by a chemical reduction method and sonication at temperature 55–65°C.

hydrazine-sodium hydroxide solution was stopped at a pH of 10 forming a gray blue solution. The $[\text{Ni}(\text{N}_2\text{H}_4)_3]\text{Cl}_2$ complex can exchange the chloride ion with the hydroxide ion to form nickel hydroxide nanoparticles, as seen in the following [18]:



X-Ray diffraction was used to analyze the structure and particle size of the powders. Figure 1(a) shows a typical XRD pattern of the Ni powder sample after sonication, filtration, and drying. The five characteristic peaks for nickel $2\theta = 44.45, 51.71, 76.41, 92.96,$ and 98.46° , corresponding to Miller indices (111), (200), (220), (311), and (222), respectively, were observed, indicating that the resulting powders are face-centered cubic (fcc) nickel (PDF #04-0850) [24]. As seen from the XRD plot, the (111) reflection is the highest intensity for the peaks. After comparing the experimental pattern to the JCPDS database (PDF #04-0850), the pattern matches a random powder arrangement for nickel. Figure 1(b) displays the result of a method matching the JCPDS file for nickel after adding a particle protector, PVP, to the solution.

The crystallite size (for particles $< 1 \mu\text{m}$) can be calculated from the line broadening in the XRD patterns. Broadening that occurs for X-ray diffraction peaks is mainly due to three factors: instrumental broadening, crystallite size, and lattice strain. Broadening due to stress follows a $\tan\theta$ function and broadening due to crystallite size follows a $1/\cos\theta$ dependence. The Williamson-Hall method can be used to determine (or separate) the contribution of each factor to the broadening of the peaks in the XRD patterns when there are three or more reflections available for measurement [25, 26]. Contributions of crystallite size and strain are given by the following equation:

$$\beta_r \cos\theta = \frac{k\lambda}{L} + \eta \sin\theta, \quad (3)$$

where λ is the wavelength of the X-rays, θ is the diffraction angle, η is the strain, L is the crystallite size, k is a constant

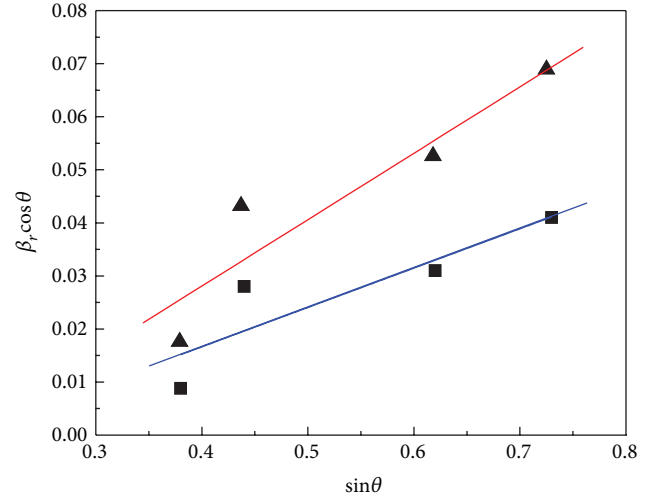


FIGURE 2: Williamson-Hall plot for XRD data of nickel powder (squares, blue line fit) and PVP-protected nickel particles (triangles, red fit lines).

(0.94 for Gaussian line profiles and small cubic crystals of uniform size), and β_r (in radians) is the corrected full width at half maximum of the peak given by

$$\beta_r^2 = \beta_m^2 - \beta_s^2, \quad (4)$$

where β_m is the experimental measured half width and β_s is the half width of a silicon powder standard with peaks corresponding to the same 2θ region. Equation (4) is used to correct for instrumental broadening, when the observed peaks have a near-Gaussian shape. From (3), a plot of $\beta_r \cos\theta$ versus $\sin\theta$ (Williamson-Hall plot) yields a straight line with a slope of η and intercept of $k\lambda/L$. For XRD patterns which exhibit preferred orientation (have fewer than 3 peaks), the Scherrer equation can be used to estimate the crystallite size [25].

Williamson-Hall plots were used to estimate nickel powder particle size for the samples (Figure 2). Broader peaks in the XRD pattern (Figure 1) of the solution that contained PVP indicated a smaller particle size, and the Williamson-Hall plot (Figure 2) confirmed that PVP-protected particles had an estimated size of 7 nm, compared to an estimate of 12 nm for non-PVP protected particles. The particle sizes between the PVP and non-PVP solution only show a small difference in values.

The precipitates of nickel hydroxide powder were similarly analyzed. A typical XRD pattern of nickel hydroxide powder is shown in Figure 3. This pattern matches the JCPDS file for $\beta\text{-Ni}(\text{OH})_2$ (PDF #14-0117) [27]. A Williamson-Hall plot of the nickel hydroxide powder (Figure 4) gives an approximate particle size of 14 nm. Table 1 lists the sizes of the synthesized powders as measured from the X-ray diffraction data.

Dynamic light scattering experiments of the colloidal solutions, before drying, were run to estimate the size of the particles in solution phase. The DLS data is listed in Table 1 and shows that the particle sizes in an aqueous solution are

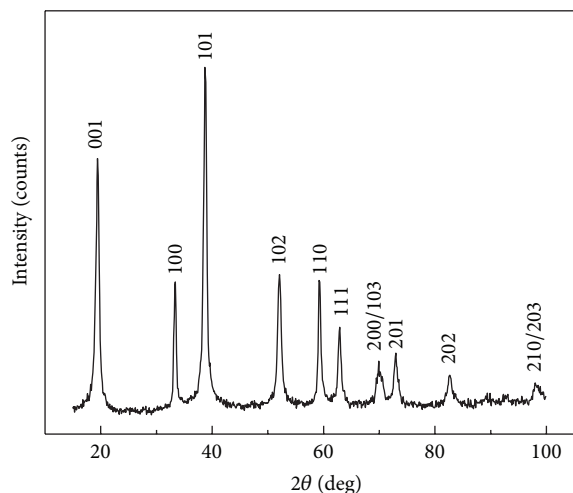


FIGURE 3: XRD pattern of precipitated nickel hydroxide powder produced by titrating nickel chloride with hydrazine-sodium hydroxide solution at pH ~ 10 .

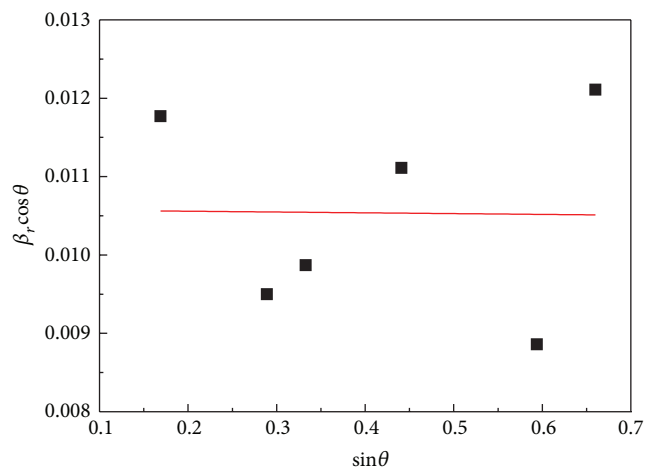
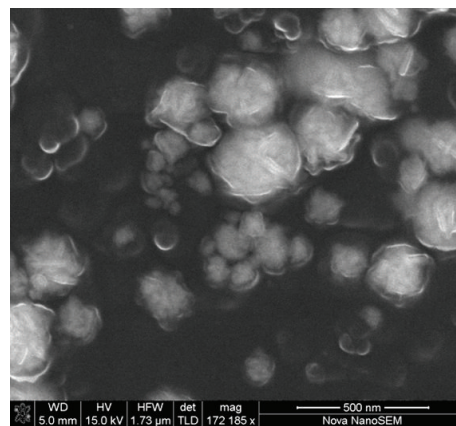


FIGURE 4: Williamson-Hall plot for XRD data of $\text{Ni}(\text{OH})_2$ synthesized powder.

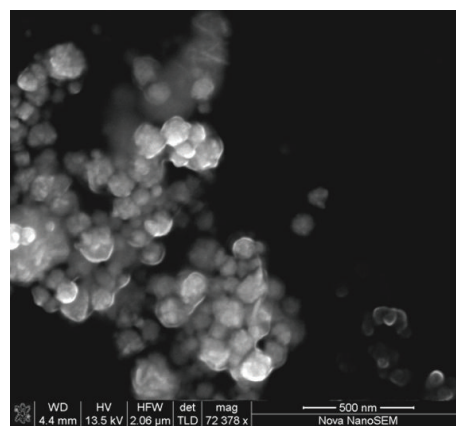
TABLE 1: Particle size of the nanopowders measured using the Williamson-Hall analysis from the X-ray diffraction data and the dynamic light scattering method.

Nanopowders	Measured particle size (nm)	
	Williamson-Hall plot	Dynamic light scattering ($n = 40$)
Nickel	12	101.7 ± 25.6
Nickel-PVP	7	25.9 ± 4.4
Nickel hydroxide	14	63.1 ± 16.2

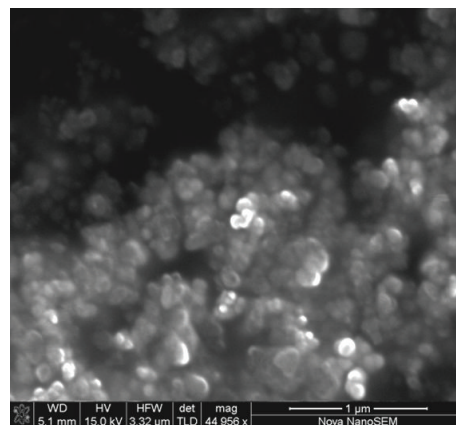
larger than the Williamson-Hall analysis of the dried powders; this is due to the agglomeration of particles in solution. The pure nickel solutions gave a value of 101.7 ± 25.6 nm and the Ni-PVP was 25.9 ± 4.4 nm. This result shows that the PVP for the synthesized nickel can help prevent agglomeration in the aqueous solution during synthesis, thus giving small



(a)



(b)



(c)

FIGURE 5: SEM images of (a) nickel, (b) Ni-PVP, and (c) $\text{Ni}(\text{OH})_2$ powder nanoparticles.

nickel nanoparticles. The $\text{Ni}(\text{OH})_2$ particle size was 63.1 ± 16.2 nm in solution also showing some agglomeration in solution. The DLS data places these particles in the nanorange while in solution, which are nanopowders when dried.

Scanning electron microscopy was also used to determine if the nanoparticles were in the nanometer range of size. Figure 5 shows the SEM image of nickel and nickel hydroxide nanoparticles produced by the simplified chemical reduction

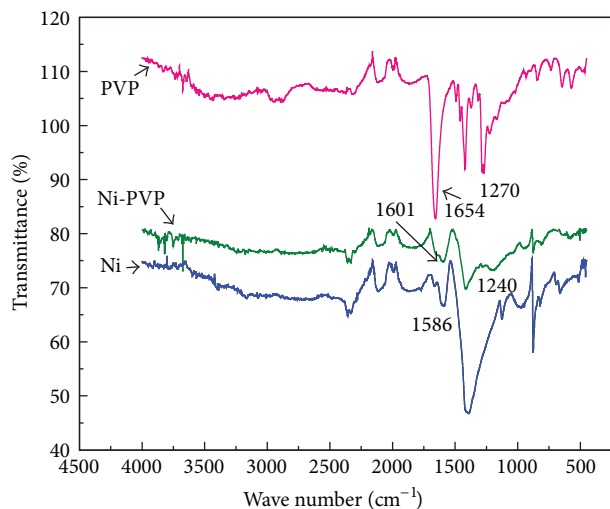


FIGURE 6: The infrared spectra of synthesized powders of pure PVP, Ni-PVP and Ni powders.

method. The measurements using the SEM were at the instruments limits of size detection; however, the image still shows that the powder particles are below 40 nm, within the nanometer range measured by XRD.

The FTIR spectra of nickel and Ni-PVP nanoparticles can be seen in Figure 6. The FTIR results show a peak at 1654 cm^{-1} for the carbonyl stretch for pure PVP. The C=O stretch red shifts from pure PVP to 1601 cm^{-1} as nickel is protected with PVP and continues to shift to pure nickel at 1586 cm^{-1} [28]. Another region to evaluate is the peaks between 1170 and 1270 cm^{-1} , which signify the C–N stretch in PVP [28]. In pure PVP, the peaks are strong with three different peaks for each of the C–N bonds in PVP. With Ni-PVP, weak shoulder peaks are seen in the region around 1240 cm^{-1} and they completely disappear with pure nickel nanoparticles. The FTIR spectrum of $\text{Ni}(\text{OH})_2$ in Figure 7 shows a hydroxyl stretch from the $\text{Ni}(\text{OH})_2$ lattice at 3629 cm^{-1} and an –O–H stretch of the intercalated hydroxyl group from water between 3100 and 3500 cm^{-1} [29, 30]. Also, an H–O–H bend is observed at 1605 cm^{-1} from the vibration of free water molecules [29]. The spectrum also shows a sharp O–H stretch at 608 cm^{-1} from the hydroxyl lattice vibration and a weak peak at 467 cm^{-1} indicating a Ni–O lattice vibration [30].

4. Conclusions

Nickel powders with nanosized particles are synthesized chemically through the reduction of a nickel salt by hydrazine hydrate in a basic aqueous solution (pH~12.5) using sonication to control the reduction at around $55\text{--}65^\circ\text{C}$. The nickel hydroxide nanopowder was precipitated by titrating nickel chloride solution with hydrazine-sodium hydroxide at a final mixture pH of ~10. The most notable features of this method are the simple operation, high yield, and small particle sizes. The procedure yields pure nanocrystalline powders with particle sizes ranging from 7 to 14 nm.

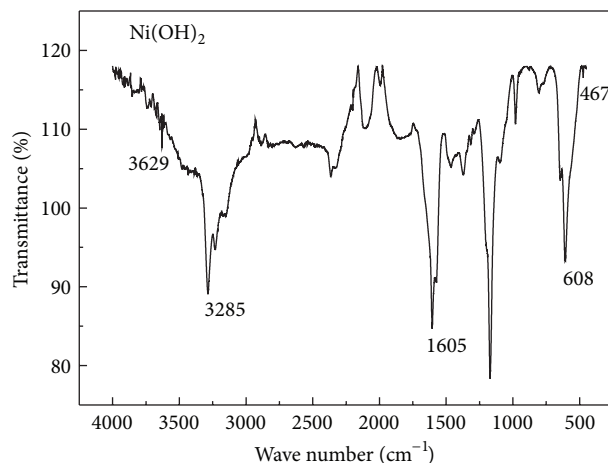


FIGURE 7: The infrared spectra of $\text{Ni}(\text{OH})_2$ powder.

Conflict of Interests

The authors declare that there is no conflict of interests regarding the publication of this paper.

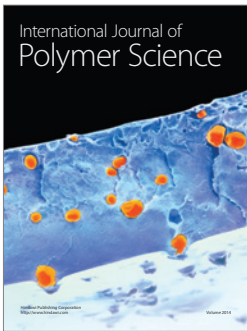
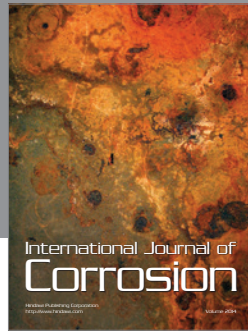
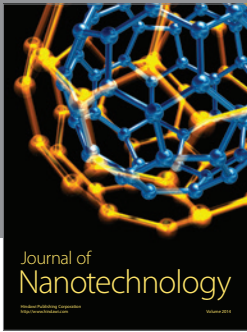
Acknowledgment

Stephanie Garcia's work was supported by the National Science Foundation under Grant no. CHE-1004878, as part of an NSF Research Experience for Undergraduates Program in the Department of Chemistry at the University of North Texas.

References

- [1] M. T. Reetz and W. Helbig, "Size-selective synthesis of nanostructured transition metal clusters," *Journal of the American Chemical Society*, vol. 116, no. 16, pp. 7401–7402, 1994.
- [2] M. Huang, Y. Shen, W. Cheng et al., "Nanocomposite films containing Au nanoparticles formed by electrochemical reduction of metal ions in the multilayer films as electrocatalyst for dioxygen reduction," *Analytica Chimica Acta*, vol. 535, no. 1-2, pp. 15–22, 2005.
- [3] B. P. S. Chauhan, J. S. Rathore, and N. G. Ilokhani, "First example of "palladium-nanoparticle"-catalyzed selective alcoholysis of polyhydrosiloxane: a new approach to macromolecular grafting," *Applied Organometallic Chemistry*, vol. 19, no. 4, pp. 542–550, 2005.
- [4] J. Zhang, X. Wang, L. Li, C. Li, and S. Peng, "Effect of reductant and PVP on morphology and magnetic property of ultrafine Ni powders prepared via hydrothermal route," *Materials Research Bulletin*, vol. 48, no. 10, pp. 4230–4234, 2013.
- [5] A. Corrias, G. Ennas, G. Licheri, G. Marongiu, and G. Paschina, "Amorphous metallic powders prepared by chemical reduction of metal ions with potassium borohydride in aqueous solution," *Chemistry of Materials*, vol. 2, no. 4, pp. 363–366, 1990.
- [6] C. Wang, X. M. Zhang, X. F. Qian, Y. Xie, W. Z. Wang, and Y. T. Qian, "Preparation of nanocrystalline nickel powders through hydrothermal-reduction method," *Materials Research Bulletin*, vol. 33, no. 12, pp. 1747–1751, 1998.

- [7] L. A. Saghatforoush, M. Hasanzadeh, S. Sanati, and R. Mehdizadeh, "Ni(OH)₂ and NiO nanostructures: synthesis, characterization and electrochemical performance," *Bulletin of the Korean Chemical Society*, vol. 33, no. 8, pp. 2613–2618, 2012.
- [8] S. Papp and I. Dékány, "Stabilization of palladium nanoparticles by polymers and layer silicates," *Colloid and Polymer Science*, vol. 281, no. 8, pp. 727–737, 2003.
- [9] P. K. Khanna and V. V. S. Subbarao, "Nanosized silver powder via reduction of silver nitrate by sodium formaldehydesulfoxylate in acidic pH medium," *Materials Letters*, vol. 57, no. 15, pp. 2242–2245, 2003.
- [10] M. Zhou, S. Chen, H. Ren, L. Wu, and S. Zhao, "Electrochemical formation of platinum nanoparticles by a novel rotating cathode method," *Physica E*, vol. 27, no. 3, pp. 341–350, 2005.
- [11] L. Rodríguez-Sánchez, M. C. Blanco, and M. A. López-Quintela, "Electrochemical synthesis of silver nanoparticles," *Journal of Physical Chemistry B*, vol. 104, no. 41, pp. 9683–9688, 2000.
- [12] M. T. Reetz, M. Winter, R. Breinbauer, T. Thurn-Albrecht, and W. Vogel, "Size-selective electrochemical preparation of surfactant-stabilized Pd-, Ni- and Pt/Pd colloids," *Chemistry*, vol. 7, no. 5, pp. 1084–1094, 2001.
- [13] H. Feng, Z. Zhengyi, X. Yaofu, W. Wuxiang, H. Yafang, and W. Run, "A new electrolytic method of preparing ultrafine metallic powders," *Journal of Materials Processing Technology*, vol. 137, no. 1–3, pp. 201–203, 2003.
- [14] W. Yu and H. Liu, "Quantity synthesis of nanosized metal clusters," *Chemistry of Materials*, vol. 10, no. 5, pp. 1205–1207, 1998.
- [15] N. Aihara, K. Torigoe, and K. Esumi, "Preparation and characterization of gold and silver nanoparticles in layered laponite suspensions," *Langmuir*, vol. 14, no. 17, pp. 4945–4949, 1998.
- [16] U. N. Tripathi, A. Soni, V. Ganesan, and G. S. Okram, "Influence of polyvinylpyrrolidone on particle size of Ni nanoparticles preparation," in *Proceedings of the 56th Dae Solid State Physics Symposium*, vol. 1447 of *AIP Conference Proceedings*, pp. 437–438, Kattankulathur, India, December 2011.
- [17] S.-H. Wu and D.-H. Chen, "Synthesis and characterization of nickel nanoparticles by hydrazine reduction in ethylene glycol," *Journal of Colloid and Interface Science*, vol. 259, no. 2, pp. 282–286, 2003.
- [18] J. W. Park, E. H. Chae, S. H. Kim et al., "Preparation of fine Ni powders from nickel hydrazine complex," *Materials Chemistry and Physics*, vol. 97, no. 2–3, pp. 371–378, 2006.
- [19] D.-P. Wang, D.-B. Sun, H.-Y. Yu, and H.-M. Meng, "Morphology controllable synthesis of nickel nanopowders by chemical reduction process," *Journal of Crystal Growth*, vol. 310, no. 6, pp. 1195–1201, 2008.
- [20] M. B. J. G. Freitas, "Nickel hydroxide powder for NiO·OH/Ni(OH)₂ electrodes of the alkaline batteries," *Journal of Power Sources*, vol. 93, no. 1–2, pp. 163–173, 2001.
- [21] D. S. Hall, D. J. Lockwood, S. Poirier, C. Bock, and B. R. MacDougall, "Raman and infrared spectroscopy of α and β phases of thin nickel hydroxide films electrochemically formed on nickel," *The Journal of Physical Chemistry A*, vol. 116, no. 25, pp. 6771–6784, 2012.
- [22] R.-Y. Chen and K.-G. Zhou, "Preparation of ultrafine nickel powder by wet chemical process," *Transactions of Nonferrous Metals Society of China*, vol. 16, no. 5, pp. 1223–1227, 2006.
- [23] D. V. Goia, "Preparation and formation mechanisms of uniform metallic particles in homogeneous solutions," *Journal of Materials Chemistry*, vol. 14, pp. 451–458, 2004.
- [24] "Joint Committee on Powder Diffraction Standard (JCPDS)," Tech. Rep. 00-004-0850, International Center for Diffraction Data (ICDD), Swarthmore, Pa, USA.
- [25] B. D. Cullity and S. R. Stock, *Elements of X-ray Diffraction*, Prentice Hall, New York, NY, USA, 3rd edition, 2001.
- [26] H. P. Klug and L. E. Alexander, *X-ray Diffraction Procedures: For Polycrystalline and Amorphous Materials*, John Wiley & Sons, New York, NY, USA, 2nd edition, 1974.
- [27] "Joint Committee on Powder Diffraction Standard (JCPDS)," Tech. Rep. 00-014-0117, International Center for Diffraction Data (ICDD), Swarthmore, Pa, USA.
- [28] G. G. Couto, J. J. Klein, W. H. Schreiner, D. H. Mosca, A. J. A. de Oliveira, and A. J. G. Zarbin, "Nickel nanoparticles obtained by a modified polyol process: synthesis, characterization, and magnetic properties," *Journal of Colloid and Interface Science*, vol. 311, no. 2, pp. 461–468, 2007.
- [29] K. Harish, R. Renu, and S. R. Kumar, "Synthesis of nickel hydroxide nanoparticles by reverse micelle method and its antimicrobial activity," *Research Journal of Chemical Sciences*, vol. 1, no. 9, pp. 42–48, 2011.
- [30] Q. Song, Z. Tang, H. Guo, and S. L. I. Chan, "Structural characteristics of nickel hydroxide synthesized by a chemical precipitation route under different pH values," *Journal of Power Sources*, vol. 112, no. 2, pp. 428–434, 2002.



Hindawi

Submit your manuscripts at
<http://www.hindawi.com>

